ANALYSIS OF INDUCED ACTIVITIES MEASUREMENTS RELATED TO DECAY HEAT IN PHASE IIC EXPERIMENTAL ASSEMBLY: USDOE /JAERI COLLABORATIVE PROGRAM ON FUSION NEUTRONICS EXPERIMENTS

A.Kumar, M.A.Abdou
School of Engineering and Applied Science
University of California at Los Angeles (UCLA)
Los Angeles,California 90024, USA

Y.Ikeda, T.Nakamura
Japan Atomic Energy Research Institute
Tokai, Ibaraki 319-11, Japan

ABSTRACT

The selection of materials and design options for fusion device components depends crucially on the level of radioactivity and decayheat induced in the components subject to D-T neutron irradiation. An experimental program was carried out to obtain decay γ emission spectra from samples of Fe, Ni, Cr, MnCu alloy, Ti, Mo, Zr, Ta, W, Si, Mg, Al, V, Nb, SS316, $YBa_2Cu_3O_7$ and $ErBa_2Cu_3O_7$, which were subjected to simulated fusion neutron environment. Cooling times obtained ranged from 10 min to 7 days. The experimental results have been analyzed using four leading radioactivity codes: DKRICF, REAC, RACC and THIDA. The integrated decay γ emission rates (over 100 KeV to 3 MeV) have been compared in addition to decay γ emission spectra. It is observed that : (i) generally, much better agreement is found between computed (C) and experimentally measured (E) values for integrated γ emission rates as against the detailed γ spectra, (ii) C/E ratios for integrated γ emission rates are found to range from 0.001 to 300, though most of the ratios cluster between 1 to 2. Significant discrepancies are obtained on C/E ratios for a number of cases for the four codes used above. Most of the observed discrepancies are due to (a) missing or wrong fundamental decay γ–ray data, e.g., (1) missing decay data in DKRICF for ^{186}Ta, ^{187}W, ^{181}W, ^{90m}Y, ^{86}Rb, ^{88}Y, etc., (2) wrong decay γ–intensities for W products in THIDA, (b) inaccurate activation cross sections, e.g., for V, Zr, Mo in DKRICF, RACC, REAC, (c) errors on computed neutron energy spectra, (d) various experiment related factors, essentially poor counting statistics for weak neutron induced reactions.

I. INTRODUCTION

Induced radioactivity level is an important parameter for characterizing design of a fusion machine. All materials used therein are subject to production of induced activity as soon as they are exposed to fusion neutrons. Currently, there is a large uncertainty associated with the activation and decay data bases of radioactivity calculation codes, e.g., DKRICF[1], RACC[2], REAC[3] and THIDA[4], due to rather narrow experimental data base for materials under consideration for fusion devices, e.g., ITER[5], NET[6] and FER[7]. An experiment to validate these codes was conducted to obtain γ-ray spectra emerging from a number of materials, e.g., Fe, Ni, Cr, Mn, Ti, Mo. Zr, Ta, W, Si, Mg, Al, V, Cu, Nb, SS316, Au, In, Mg, Al, Nb, Ta, $YBa_2Cu_3O_7$ and $ErBa_2Cu_3O_7$, which were subjected to simulated fusion neutron environment[8-9]. Of these, $YBa_2Cu_3O_7$ and $ErBa_2Cu_3O_7$ (on substrate of yttria stabilized zirconia) are known high temperature superconductors, and Au, In, Mg, Fe, Al, Nb, and Ta were also intended to serve as dosimetry foils for monitoring neutron energy spectrum. The experiment was performed during phase IIC of USDOE/JAERI collaborative program on fusion neutronics. Samples of different materials were irradiated at two locations, at 10 and 82 cm from target, inside coolant channel assembly of phase IIC[10-11]. Figure 1 shows the schematic of the arrangement.

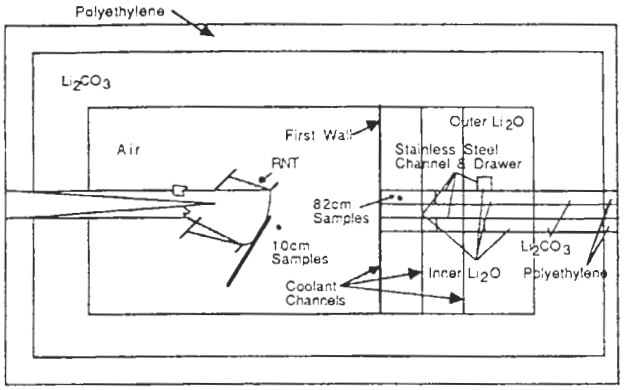

Figure 1: Schematic arrangement of samples in Phase IIC coolant channel assembly.

Two separate irradiation programs were executed to cover each of the two locations. Two foil packets were irradiated at each location to individually focus on: (i)shorter half life products (less than 1 hour half life), (ii)longer half life products (1 hour to 5 year half life). Each irradiation program consisted of initial half an hour irradiation followed by pulling out of one of the two packets. The γ-spectroscopy of the foils in this packet was to cover primarily shorter half life products. The total irradiation periods were 9 and 10 hours respectively for the locations at 10 and 82 cm, logging average source neutron intensities of $8.75.10^{11}$ and $1.12.10^{12}$ n/s. The γ-spectroscopy of each sample was done using four intrinsic germanium detectors and for multiple cooling periods ranging from 20 m to 10 d. Three detectors were relatively calibrated with respect to an absolutely calibrated standard detector.

The experimental data was treated to obtain spectra of decay γ emission rate per g of the irradiated specimen (see Section II). These quantities were also computed using leading radioactivity calculation packages: DKRICF, REAC,

RACC, THIDA (Section III). The measured and computed decay γ-emission rates were then intercompared (Section IV).

II. TREATMENT OF EXPERIMENTAL DATA

Figure 2 is a flow diagram depicting what is broadly involved in intercomparison of measured and computed decay γ spectra. γ pulse-height spectrum for a sample for a each cooling time is processed by a spectrum analysis code BOB75[12] to obtain gamma ray intensity spectrum. Then background is subtracted. The resulting spectrum is then corrected for detector efficiency and attenuation of decay γ's emitted in a sample. Variation of source neutron intensity during irradiation is accounted for to finally obtain decay γ emission rate per g for a normalizing source neutron intensity of 10^{12} n/s. It is to be added that standard deviation on each γ-peak is a function of many parameters, e.g., neutron flux, counting time, waiting time, counting efficiency, activation cross-section, half-life of γ-peak emitter, γ-yield etc. It is insufficient to characterize this standard deviation by a single factor, even as, γ-emitters with longer half lives can be expected to carry larger errors. It is interesting to look at Fig. 3 that shows % standard deviation as a function of product half life for a nickel sample irradiated at 10 cm distance from target for 9 hours. It is hard to extract any systematic trends as a function of a single parameter as already outlined earlier.

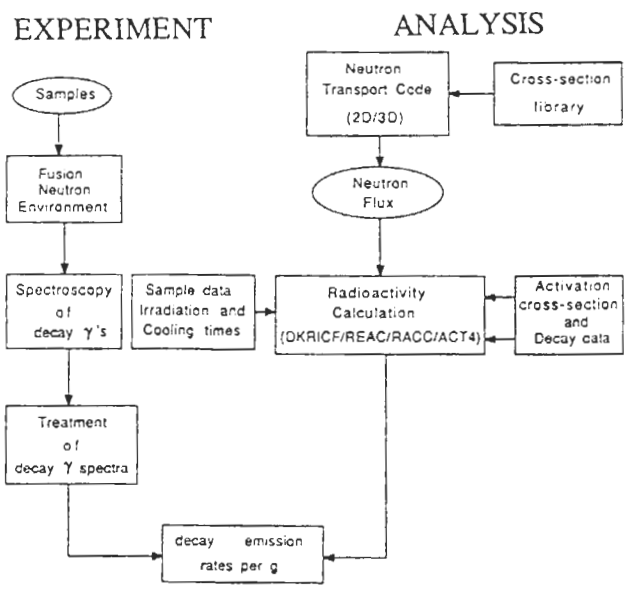

Figure 2: Flow chart of experiment and calculation.

III. ANALYSIS

As shown in Figure 2, analysis to obtain decay γ emission rate involves a multi-step procedure. A two or three dimensional transport code is employed to get neutron energy distribution, i.e.,neutron flux, at spatial locations of samples. Geometry and material composition of irradiation environment are important inputs for this calculation. Next stage involves computation of decay γ emission spectrum

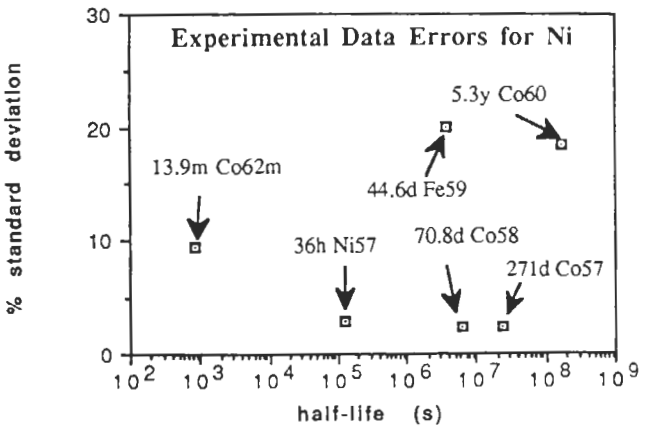

Figure 3: Percent Standard deviation on measured decay γ emission rate as a function of product half life for a nickel sample

Table 1

Radioactive Products from Stainless Steel and Tungsten Samples

(3m < half life < 5 y)

Sample-material	Half-life	Product	γ-energy (dominant)	Reaction
SS316	3.76 m	^{52}V	1434 KeV	^{55}Mn(n,α); ^{52}Cr(n,p)
	5.8 m	^{51}Ti	320 KeV	^{54}Cr(n,α)
	8.5 m	^{53}Fe	378 KeV	^{54}Fe(n,2n)
	10.5 m	^{60m}Co	58.6 KeV	^{60}Ni(n,p)
	13.9 m	^{62}Co	1173 KeV	^{62}Ni(n,p)
	14.6 m	^{101}Mo	192 KeV	^{100}Mo(n,γ)
	15.5 m	^{91}Mo	1634 KeV	^{92}Mo(n,2n)
	41.9 m	^{49}Cr	91 KeV	^{50}Cr(n,2n)
	51.5 m	^{98m}Nb	723/787 KeV	^{100}Mo(n,t),^{98}Mo(n,p)
	72 m	^{97}Nb	658 KeV	Mo(n,p), (n,n'p),(n,d)
	1.65 h	^{61}Co	67 KeV	Ni(n,n'p), (n,α)
	2.52 h	^{65}Ni	1482 KeV	^{64}Ni(n,γ)
	2.58 h	^{56}Mn	847 KeV	^{56}Fe(n,p);^{55}Mn(n,γ)
	16.9 h	^{97}Zr	743 KeV	^{100}Mo(n,α)
	23.4 h	^{96}Nb	569/778 KeV	Mo(n,p),(n,n'p)
	36 h	^{57}Ni	1373 KeV	^{58}Ni(n,2n)
	78.4 h	^{89}Zr	909 KeV	^{92}Mo(n,α)
	10.14 d	^{92m}Nb	935 KeV	^{92}Mo(n,p)
	15.97 d	^{48}V	984 KeV	^{50}Cr(n,t)
	27.7 d	^{51}Cr	320 KeV	^{54}Fe(n,α);^{52}Cr(n,2n)
	44.6 d	^{59}Fe	1099 KeV	^{62}Ni(n,α)
	70.8 d	^{58}Co	811 KeV	^{58}Ni(n,p)
	271 d	^{57}Co	122 KeV	^{58}Ni(n,n'p),(n,d)
	312.2 d	^{54}Mn	835 KeV	^{54}Fe(n,p); ^{55}Mn(n,2n)
	5.27 y	^{60}Co	1332 KeV	^{60}Ni(n,p)
W	10.5 m	^{186}Ta	198 KeV	^{186}W(n,p)
	49.5 m	^{185}Ta	178 KeV	^{186}W(n,n'p), (n,d)
	64 m	^{183}Hf	784 KeV	^{186}W(n,α)
	23.9 h	^{187}W	480 KeV	^{186}W(n,γ)
	5 d	^{183}Ta	246 KeV	^{183}W(n,p)
	115 d	^{182}Ta	1121 KeV	^{182}W(n,p)
	121 d	^{181}W	136 KeV	^{180}W(n,γ)

using a radioactivity calculation code. Neutron flux, sample composition, irradiation and cooling (or shutdown) times are required input data for this stage. Decay and activation cross-section libraries form part of the code used. Leading codes used for this purpose include DKRICF, REAC, RACC and THIDA. In fact, THIDA is a code system that includes neutron flux calculating modules too. However, its central module is ACT4 that calculates induced radioactivity and associated quantities.

Table 2
Chemical Composition of Primary Impurities in the Samples Used in Induced Activity Irradiations of December, 1988

Sample Material	Chemical Composition by Maximum weight %
Iron (Fe)	99.92 Fe, 0.059 Mn, 0.02 C
Nickel (Ni)	99.97 Ni, 0.016 C
Molybdenum (Mo)	99.93, 0.03 W, 0.01 Fe
Stainless Steel@ (SS316)	66.22 Fe, 17.75 Cr, 11.60 Ni, 2.08 Mo, 1.33 Mn, 0.42 Si, 0.19 Co, 0.34 Cu, 0.06 V
Manganese Copper Alloy+ (MnCu)	79.78 Mn, 19.66 Cu, 0.46 Ni, 0.07 Fe
Vanadium (V)	99.82 V, 0.044 Si, 0.03 Ta, 0.03 O, 0.013 Mo, 0.01 Zr, 0.01 Fe, 0.01 Al, 0.01 Hf
Titanium (Ti)	99.79 Ti, 0.12 O, 0.06 Fe, 0.02 C
Aluminum (Al)	99.97 Al, 0.006 Mg
Cobalt (Co)	99.95 Co, 0.04 Ni
Tungsten (W)	99.97 W, 0.008 Si
Niobium (Nb)	99.91 Nb, 0.018 Ta, 0.01 Zr
Zirconium (Zr)	99.76 Zr, 0.10 Fe, 0.09 Si, 0.03 Ti
Indium (In)	99.99 In, 0.003 Cu
Tantalum (Ta)	99.98 Ta, 0.007 Fe
Magnesium (Mg)	99.78 Mg, 0.10 Al, 0.07 Zr, 0.02 Mn, 0.01 Si

Two calculational schemes were followed for analysis. First scheme related to use of externally evaluated neutron flux with four radioactivity codes: DKRICF, REAC, RACC and ACT4. The flux was obtained in a two step process: (1)source neutron energy and angular distribution was obtained by 3D MCNP[13] modeling of rotating neutron target (RNT) of fusion neutronics source (FNS) facility , (2)source neutron distribution from MCNP was input to RUFF[14] and DOT4.3[15] code system to compute spatial distribution of neutron flux. 30 group MATXS5 cross-section library of LANL was used for neutron transport. The neutron flux was also obtained by full-fledged MCNP caculation and was found to match the flux via the foregoing approach. As neutron energy group boundaries are different for the radioactivity codes used, flux transformation from one group structure to another was carried out subject to total neutron flux conservation. It is evident that this will add to total numerical error entailed in decay rate computation. However, it should not amount to more than a percent for most of the cases. The second calculational scheme is similar to the one in reference 16, wherein THIDA code is employed for whole analysis.

Multitude of neutron induced reactions and range of product half lives can be gauged from Table 1 which lists γ-emitting radioactive products, of half life from 3m to 5y, for stainless steel and tungsten samples. Primarily, dominant γ-energies are shown. In all, more than 150 γ-emitting products are of interest, covering all samples. Table 2 lists compositions of various foil materials. These compositions have been provided by commercial suppliers of these samples.

IV. RESULTS AND DISCUSSION

Tables 3a to 3d summarize results of comparison of integrated, from 100 KeV through 3 MeV, decay γ-emission rates per g normalized to source intensity of 10^{12} n/s. The computed results from REAC-2, DKRICF and THIDA-2 are included. RACC results generally follow same trends as those from DKRICF, though spectral distributions of decay γ-emission rates differ at times. Large deviations in C/E (Computed/Experimental) ratio are observed for Mo, W, MnCu alloy, Cr, Zr, Ta and $YBa_2Cu_3O_7$. Tables 3a to 3c show upper and lower bounds of C/E ratios for integrated decay emission rates for the three codes as a function of irradiated material. Though C/E ratios for Fe, Ni, Mo, SS316 and many other materials behave reasonably well, large discrepancies are seen for spectral distributions. Figures 5a to 5f typically bring home this aspect. The materials covered include Iron, Nickel, Molybdenum, Stainless Steel (SS316) and Tungsten. The experimental data displayed is of two kinds: energy-group integrated for direct comparison, and gamma-ray peak-wise data for detailed break-down. tr and tcool respectively stand for irradiation and cooling times.Table 4 lists important radioactive products and gamma rays observed during measurements for some of the materials. Specific observations follow for few materials.

IV.A. Iron

^{56}Mn dominates for short cooling times, ^{54}Mn takes over at longer cooling times; other contributors include ^{51}Cr and ^{58}Co (nickel impurity). Some samples showed also presence of nickel/aluminum/magnesium impurities. REAC and ACT4 (a component module of THIDA) have, generally, more reliable γ-emission data. RACC cross-section data for ^{56}Fe(n,p)^{56}Mn are closest to published experimental ones. γ-yield data is generally the lowest for ACT4 even as the activation cross-sections are quite close to others. DKRICF lacks γ-yield data for gamma-rays carrying more than 2.5 MeV. In spite of all these differences, the evaluated and measured reaction rates for ^{56}Mn, ^{54}Mn and ^{51}Cr agree within 15%, even though, the softer spectrum, at distance of 82 cm from target, tends to raise C/E ratios.

IV.B. Nickel

^{62m}Co and ^{57}Ni dominate at short cooling times. At longer cooling times, ^{58}Co, ^{57}Co, ^{57}Ni, ^{59}Fe, ^{60}Co dominate. REAC strongly overestimates (by at least a factor of 2) contributions from ^{58}Co and ^{59}Fe. Also ^{57}Co is overestimated by as much as 25%. C/E for ^{57}Co for DKRICF is in the range of 0.97 to 1.08 for all cases; C/E for ^{58}Co ranges from 0.0.97 to 1.24; C/E for ^{59}Fe is 0.82 for DKRICF as against 2.61 for REAC2; C/E for ^{60}Co is 0.83 as against 1.63 for REAC2.

IV.C. Molybdenum

For short cooling times, ^{97}Nb, ^{98m}Nb, ^{99}Mo,^{99m}Tc, ^{96}Nb, ^{101}Mo, ^{101}Tc, ^{93m}Mo and ^{91}Mo contribute predominantly. ^{99m}Tc and ^{101}Tc respectively result from β$^-$ decays of ^{99}Mo and ^{101}Mo. Longer cooling times see dominance of ^{99}Mo, ^{99m}Tc, ^{96}Nb, ^{97}Nb and ^{89}Zr. ^{91}Mo

Table 3a
Comparison of Measured and Computed Decay γ Emissions/s/g of Material per 10^{12} source neutron/s

Material	Distance from Source	Irradiation Time	Cooling Time	Counting Time	C/E REAC-2	C/E DKRICF	C/E THIDA
Fe	10 cm	30 m	22.4 m	10 m	0.85	0.98	0.91
	10 cm	9 h	3h 22.3m	22.4 m	1.00	1.17	1.06
	10 cm	9 h	5d 13.7h	5h 16.9m	0.95	1.00	1.02
	82 cm	30 m	24.0 m	10 m	1.10	1.22	1.06
	82 cm	10 h	5h 1m	44.8 m	1.01	1.13	- - -
	82 cm	10 h	17h16.2m	39.8 m	0.98	1.14	0.97
Ni	10 cm	30 m	56.3 m	30.9 m	1.10	1.18	0.88
	10 cm	9 h	2h 26.7m	42.9 m	1.13	1.24	1.01
	10 cm	9 h	16h 23.7m	44.7 m	1.17	1.24	1.01
	10 cm	9 h	4d 13h	8h 41.9m	1.30	1.04	- - -
	82 cm	30 m	58.8 m	26.6 m	1.89	2.02	1.17
	82 cm	10 h	3h 52.7m	1h 2.8m	1.12	1.20	0.88
	82 cm	10 h	2d 17.6h	4h 13.2m	1.39	1.23	1.09
Mo	10 cm	30 m	46.3 m	30.5 m	6.99	2.55	1.22
	10 cm	9 h	1h 38.2m	43.8 m	2.09	1.55	1.51
	10 cm	9 h	15h 11.8m	1h 5.5m	1.21	1.22	1.21
	10 cm	9 h	19h 42.3m	2h 46.7m	1.37	1.42	1.14
	10 cm	9 h	4d 3.7h	15h 28.6m	1.18	1.22	- - -
	82 cm	30 m	58.8 m	26.6 m	3.39	1.85	1.11
	82 cm	10 h	2h 28.5m	38.2 m	5.40	1.26	- - -
	82 cm	10 h	9h 15.8m	4h 2.2m	3.57	1.41	- - -
SS316	10 cm	30 m	37.3 m	14.6 m	0.86	0.95	0.98
	10 cm	9 h	1h 38.8m	42.4 m	0.92	1.06	0.92
	10 cm	9 h	4h 31m	2h 46.7m	1.04	1.20	0.97
	10 cm	9 h	15h 16.8m	1h 0.5m	1.14	1.23	0.98
	10 cm	9 h	3d 21.8h	13h 54.6m	1.35	1.15	- - -
	82 cm	30 m	39.2 m	15.1 m	1.11	1.16	1.15
	82 cm	10 h	3h 13.2m	33.9 m	0.84	0.88	0.94
	82 cm	10 h	1d15h53m	21h 48.8m	1.24	1.16	0.79

Table 3b
Comparison of Measured and Computed Decay γ Emissions/s/g of Material per 10^{12} source neutron/s

Material	Distance from Source	Irradiation Time	Cooling Time	Counting Time	C/E REAC-2	C/E DKRICF	C/E THIDA
Nb	10 cm	9 h	4h 31m	2h 46.7m	1.27	0.87	0.75
	10 cm	9 h	18h 49.5m	44.5 m	1.09	1.05	0.88
	82 cm	10 h	13h 39m	1h 13.7m	1.25	1.13	0.82
Co	10 cm	30 m	37.3 m	15 m	0.84	1.03	0.85
	10 cm	9 h	3h 17.2m	29.2 m	1.40	1.27	1.11
	10 cm	9 h	17h 15.7m	40.5 m	2.13	1.24	1.11
	10 cm	9 h	5d19h9m	3h 21.5m	2.10	1.23	- - -
	82 cm	30 m	39.3 m	15.1 m	1.51	1.58	1.23
	82 cm	10 h	3h 53m	1h 2.7m	1.40	1.16	- - -

Table 3c
Comparison of Measured and Computed Decay γ Emissions/s/g of Material per 10^{12} source neutron/s

Material	Distance from Source	Irradiation Time	Cooling Time	Counting Time	C/E REAC-2	C/E DKRICF	C/E THIDA
V	10 cm	30 m	22.3 m	10 m	1.06	1.35	0.90
	10 cm	9 h	3h 42.2m	36.1 m	1.57	3.38	1.59
	10 cm	9 h	17h 16.2m	39.8 m	1.55	3.35	1.59
	82 cm	30 m	24 m	10 m	1.31	1.81	1.09
	82 cm	10 h	5h 1.7m	44.9 m	1.44	3.18	1.40
	82 cm	10 h	2d22h26m	14h 51.3m	1.41	3.11	1.20
Ti	10 cm	30 m	22.3 m	10 m	1.69	1.24	0.72
	10 cm	9 h	3h 51.5m	29.2 m	1.28	1.15	0.74
	10 cm	9 h	18h 11m	1h 20.5m	1.16	1.12	- - -
	82 cm	30 m	24.3 m	10 m	1.73	1.62	0.58
	82 cm	10 h	7h 27.5m	1h 43.4m	1.24	1.43	0.67
W	10 cm	30 m	37.3 m	15.5 m	3.07×10^{2}	0.20	0.99*(2.19)
	10 cm	9 h	2h 26.5m	44.2 m	2.55	2.86×10^{-2}	0.82*(2.38)
	10 cm	9 h	16h 23.4m	45.7 m	2.28	1.27×10^{-2}	0.76*(2.38)
	10 cm	9 h	2d19h3.5m	18h 22.7m	2.05	4.05×10^{-2}	0.70*(2.26)
	82 cm	30 m	39.2 m	15.1 m	1.38×10^{1}	7.00×10^{-3}	0.65*(2.11)
	82 cm	10 h	3h 13.5m	33.5 m	2.26	4.88×10^{-4}	0.96*(3.17)
	82 cm	10 h	4d 5.3m	13h 32.2m	2.59	2.35×10^{-3}	0.91*(2.99)
Zr	10 cm	30 m	56.5 m	18.9 m	4.13	0.82	1.21
	10 cm	9 h	2h 26.5m	43.5 m	5.58	1.08	- - -
	10 cm	9 h	17h 15.7m	40.0 m	5.81	1.16	- - -
	82 cm	30 m	58.3 m	27.1 m	4.30	0.88	1.13
	82 cm	10 h	3h 13.5m	33.7 m	4.10	0.83	1.31
MnCu	10 cm	30 m	12.3 m	10 m	3.35	3.42	1.04
	10 cm	9 h	2h 26.7m	44.0 m	1.75	1.19	0.83
	10 cm	9 h	16h 23.7m	45.7 m	1.21	0.29	0.26
	10 cm	9 h	6d20h59m	4h 50.3m	1.09	1.11	- - -
	82 cm	30 m	24.3 m	10 m	2.52	2.42	1.49
	82 cm	10 h	3h 52.7m	1h 2.2m	2.19	2.03	1.40
	82 cm	10 h	3d13h28m	6h 44.9m	1.24	1.00	0.80
Cr	10 cm	9 h	1h 38.8m	43.0 m	2.95	1.35	0.55
	10 cm	9 h	15h 16.8m	1h 0.5m	1.54	1.05	0.88
	82 cm	10 h	2h 27.5m	1h 19.6m	2.95	1.67	0.64

*several γ-rays 'unreasonably' overestimated in the library are suppressed

contribution is strongly overestimated by REAC. C/E ratios for this isotope are 328 and 307 respectively in 1.5-2 and 2.5-3 MeV ranges respectively. Other products are strongly underestimated by REAC. It is seen from experimental data that ratio of γ-yields for 778 to 569 KeV peaks from ^{96}Nb is 3.1 instead of 1.74 (see ref. 17); it is to be added here that quite possibly the balance of contribution for 778 KeV peak pertains to 66h ^{99}Mo. Respective C/E ratios for different products for REAC2 and DKRICF are: (1)^{93m}Mo: 200/1.11, (2)^{96}Nb: 2.04/3.49, (3)^{99}Mo: 1.08/1.11, (4)$^{89m+g}$Zr: 6/1.35, (5)^{97}Nb: 2.68/2.57, (6)^{95}Nb: 2/2.5, (7)^{95m}Nb: 0.77/0.20, (8)^{92m}Nb: 0.90/0.90, (9)^{95}Zr: 0.87/0.86.

IV.D. MnCu Alloy

^{56}Mn, ^{62}Cu, ^{52}V, ^{62m}Co and ^{65}Ni are most important contributors for short cooling times. ^{54}Mn dominates larger cooling times. 511 KeV γ from ^{62}Cu is overestimated by a factor of more than 3 by REAC2 and DKRICF. C/E ratios are found considerably larger than 1 for ^{56}Mn. In fact, even for other materials, there is a general trend for the codes to predict larger C/E ratios for (n,γ) reactions in presence of softer neutron energy spectrum (at 82 cm from target). REAC gives C/E ratios close to 1 for ^{54}Mn. DKRICF and REAC generally agree between themselves from 0.1 to 2.5 MeV.

Table 3d
Comparison of Measured and Computed Decay γ Emissions/s/g of Material per 10^{12} source neutron/s

Material	Distance from Source	Irradiation Time	Cooling Time	Counting Time	C/E REAC-2	C/E DKRICF	C/E THIDA
Al	10 cm	30 m	1h 15.8m	11.4 m	0.98	1.02	1.17
	10 cm	9 h	4h 31m	2h 46.7m	0.88	0.92	1.06
	82 cm	30 m	58.3 m	27.1 m	1.34	1.39	1.05
	82 cm	10 h	5h 52.3m	1h 28.5m	1.03	1.07	1.12
Si	10 cm	30 m	37.3 m	15 m	2.80	1.08	1.14
Mg	10 cm	9 h	3h 51.7m	26.3 m	1.16	1.07	0.99
	10 cm	9 h	18h 11.7m	31.5 m	1.08	1.00	---
	82 cm	10 h	5h 2m	44.2 m	1.37	1.28	1.25
In	10 cm	9 h	1h 38.2m	42.9 m	1.06	1.08	---
	10 cm	9 h	16h 23.7m	45.7 m	2.62	0.18	---
	82 cm	10 h	2h 28.5m	38 m	1.11	1.52	---
Ta	10 cm	9 h	3h 17.2m	28.2 m	3.67	0.35	---
	10 cm	9 h	18h 11.7m	35.4 m	2.03	0.83	---
	82 cm	10 h	3h 53m	1h 2.7m	1.74	1.53	0.19
Au-thick	10 cm	9 h	3h 51.7m	25.9 m	1.71	0	---
	10 cm	9 h	18h 49.5m	43.7 m	2.16	0	---
	82 cm	10 h	5h 2m	44.2 m	6.43	0	---
Au-thin	10 cm	9 h	4h 31m	2h 46.7m	1.33	0	---
	10 cm	9 h	19h 42m	2h 46.7m	1.57	0	---
$YBa_2Cu_3O_7$	10 cm	30 m	1h 32m	2h 32.9m	0.97	0.31	---
	10 cm	30 m	4h 12m	4h 31.2m	0.73	4.38×10^{-2}	---
	10 cm	30 m	7d2h26.1m	2h 50.4m	0.72	1.30×10^{-3}	---
$ErBa_2Cu_3O_7$	10 cm	30 m	1h 33m	2h 34.3m	6.20	1.06	---
	10 cm	30 m	4h 12.5m	4h 33.5m	7.69	1.30	---
	10 cm	30 m	11d4h47m	3h 34.7m	0.58	0.12	---

IV.E. Chromium

Dominant contributors are ^{51}Cr and ^{49}Cr. 847 and 1811 KeV peaks of ^{56}Mn are also detected- Fe/Mn impurity is expected. Unidentified peaks at 147, 563, 573 and 601 KeV were observed. ^{48}V contribution was absent. However, REAC predicts a large contribution from this isotope; γ-yield data appears acceptable. As a result, C/E (=6.2) is strongly overpredicted in 0.4-1 MeV range. DKRICF has C/E of 2.2 for the same range. REAC yields C/E of 2.63 for ^{49}Cr, whereas DKRICF yields a value of 0.96.

IV.F. Stainless Steel (SS316)

^{56}Mn contributes overwhelmingly at short cooling times. At larger cooling times, ^{99}Mo, ^{99m}Tc, ^{51}Cr, ^{58}Co, ^{57}Ni, and ^{54}Mn are leading contributors. C/E trends for individual contributors are same as discussed before for Fe, Ni, Cr and Mo.

IV. G. Vanadium

Short cooling times bring leading contibutions from ^{51}Ti, ^{52}V and ^{48}Sc. Larger cooling times bring out total dominance of ^{48}Sc. C/E ratios, from REAC, are 1.01 and 0.86 respectively for ^{51}Ti and ^{52}V at 10 cm location. C/E ratio of 1.5 is found for the same location for ^{48}Sc by the same code. For DKRICF, C/E for ^{48}Sc is ~3.

IV. H. Zirconium

^{89}Zr, ^{87m}Sr, ^{90m}Y, ^{94}Y, ^{92}Y and ^{91}Sr contribute at short cooling times. Larger cooling times bring out predominance of ^{89}Zr and ^{90m}Y. REAC largely overpredicts C/E (factor of 4 to 5) for both ^{89}Zr and ^{90m}Y. For ^{91m}Y, C/E is 1.7. However, C/E for ^{87m}Sr is close to 1 for REAC and is just 0.4 for DKRICF. Nevertheless, DKRICF has good agreement with the experimental data otherwise.

Table 4:

Important Radioactive Products and Prominent Gamma-ray Peaks

Irradiated Material	Products/γ-ray peaks
Fe	8.5m ^{53}Fe: 378 KeV 2.6h ^{56}Mn: 847/1811/2113/2523/2658/2960/3370 KeV 27.7d ^{51}Cr: 320 KeV 44.6d ^{59}Fe: 143/192/334.8/1099/1292 KeV 312.2d ^{54}Mn: 835 KeV
Cr	41.9m ^{49}Cr: 91/153/1362/1423/1508/1515/1570 KeV 15.97d ^{48}V: 984/1312/2240 KeV 27.7d ^{51}Cr
Ni	13.9m ^{62m}Co: 778/875/1129/1164/1173/1719/2004/2105 KeV 2.5h ^{65}Ni: 366/1116/1482/1623/1725 KeV 36h ^{57}Ni: 127/1377/1757/1919 KeV 44.6d ^{59}Fe: 143/192/1099/1292 KeV 70.8d ^{58}Co: 811/864/1674 KeV 271d ^{57}Co: 122/137/692 KeV 5.27y ^{60}Co: 1173/1332 KeV
MnCu alloy	8.76m ^{52}V: 1332/1434/1531 KeV 9.8m ^{62}Cu: 511/876/1173 KeV 13.9m ^{62m}Co, 2.6h ^{56}Mn, 2.52h ^{65}Ni 12.9h ^{64}Cu: 1346 KeV 312.2d ^{54}Mn, 5.27y ^{60}Co
Mo	14.2m ^{101}Tc: 127/184/307/545 KeV 14.6m ^{101}Mo: 192/409/506/591/696/934/1013/1161/1251/2032 KeV 15.5m ^{91}Mo: 1582/1634/2632 KeV 51.5m ^{98m}Nb: 173/355/645/714/723/787/792/824/834/996/1169/1432/1511 KeV 72m ^{97}Nb: 658/1025/1269/1516 KeV 6.95h ^{93m}Mo: 263/685/1477 KeV 16.9h ^{97}Zr: 355/508/743/1148 KeV 23.4h ^{96}Nb: 460/569/778/1091/1200 KeV 66h ^{99}Mo: 141/181/366/739/778 KeV 6.02h ^{99m}Tc: 141 KeV 78.4h ^{89}Zr: 909/1621/1657/1713/1745 KeV 87h ^{95m}Nb: 204/786 KeV 10.14d ^{92m}Nb: 913/935/1848 KeV 35d ^{95}Nb: 766 KeV 64d ^{95}Zr: 724/757 KeV

Table 4 (Continued)

W	10.5m ^{186}Ta: 122/198/215/274/308/418/615/738 KeV 64m ^{183}Hf: 459/398/784/1470 KeV 23.9h ^{187}W: 134/480/552/618/689/773 KeV 5d ^{183}Ta: 246/354 KeV 115d ^{182}Ta: 155/222/230/264/266/1121/1189/1221/1231/1257 KeV
Ta	5.5h ^{180m}Hf: 93/215/332/443/501 KeV 8h ^{180m}Ta: 93/103 KeV 115d ^{182}Ta
Zr	18.7m ^{94}Y: 551/919/1139 KeV 49.7m ^{91m}Y: 556 KeV 72m ^{97}Nb: 658 KeV 2.81h ^{87m}Sr: 388 KeV 3.19h ^{98m}Y: 203/480 KeV 3.54h ^{92}Y: 449/935/1405 KeV 9.48h ^{91}Sr: 556/653/750/1024 KeV 16.9h ^{97}Zr: 743 KeV 78.4h $^{89m+g}$Zr: 909/1713 KeV 64d ^{95}Zr: 724/757 KeV
Ti	5.8m ^{51}Ti: 320/609/929 KeV 3.1h ^{45}Ti: 720 KeV 3.9h ^{44}Sc: 1157 KeV 43.7h ^{48}Sc: 175/984/1038/1213/1312 KeV 3.42d ^{47}Sc: 159 KeV 83.8d ^{46}Sc: 889/1121 KeV

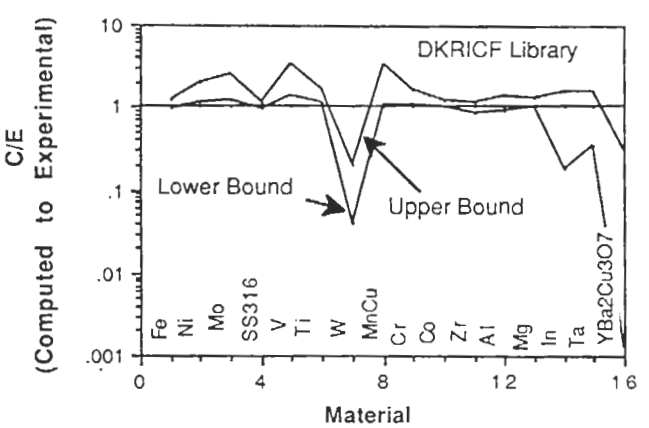

Figure 4a: Measured and DKRICF computed decay γ integrated decay rate: Comparison

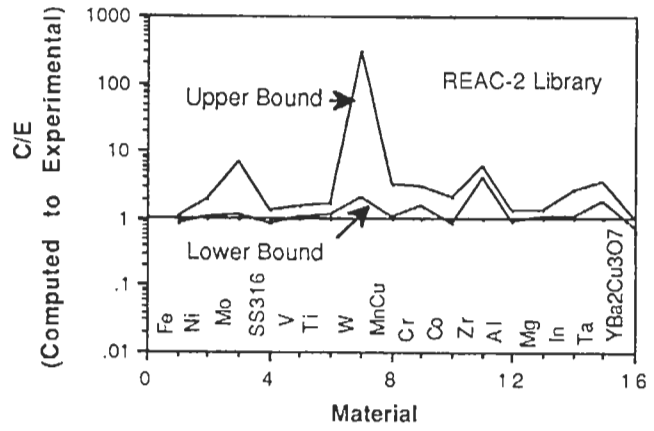

Figure 4b: Measured and REAC-2 computed decay γ integrated decay rate: Comparison

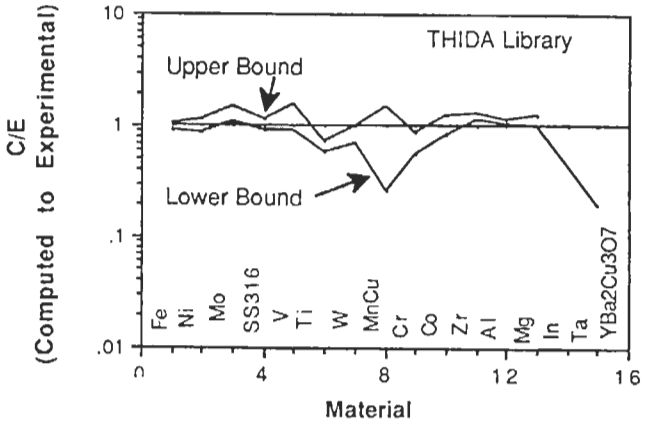

Figure 4c: Measured and THIDA-2 computed decay γ integrated decay rate: Comparison

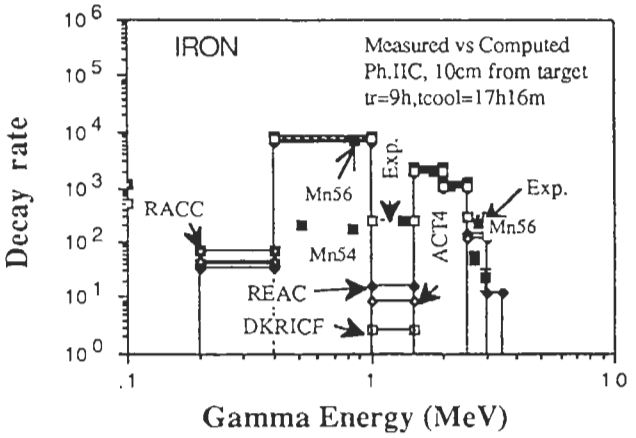

Figure 5a: Decay γ-emission rate spectrua per g for Iron: Measurement vs. Computation (tr = 9h, tcool = 17h16m)

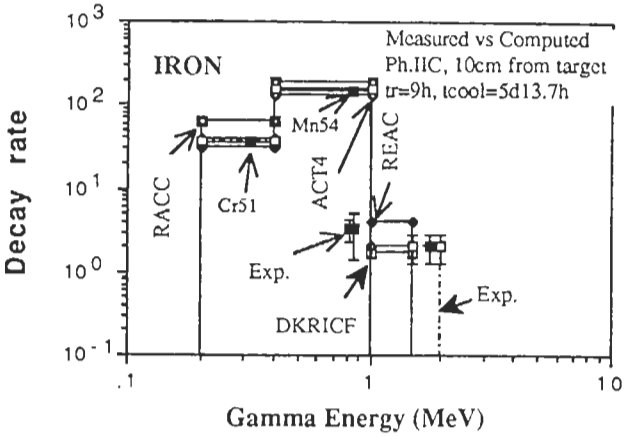

Figure 5b: Decay γ emission rte spectra per g from Iron (Cooling time = 5d13.7h): Measurement vs. Computation (tr = 9h)

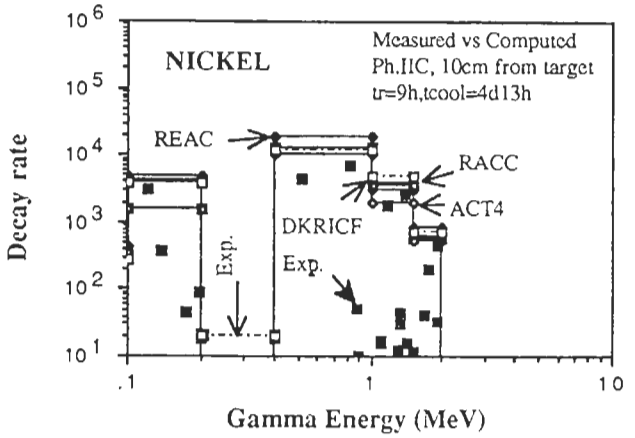

Figure 5c: Decay γ emission rate spectra per g from Nickel: Measurement vs. Computation (tr = 9h, tcool = 4d13h)

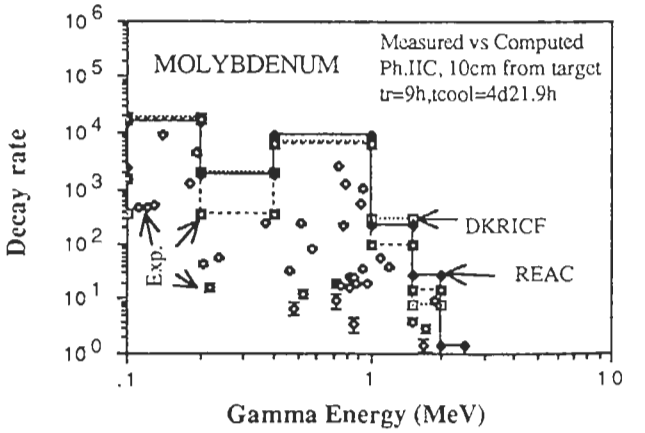

Figure 5d: Decay γ emission rate spectra per g from Molybdenum: Measurement vs. Computation (tr = 9h, tcool = 4d21.9h)

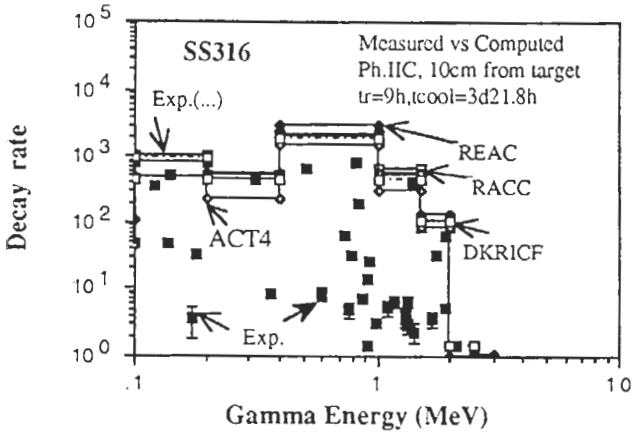

Figure 5e: Decay γ emission rate spectra per g from Stainless Steel: Measurement vs. Computation (tr = 9h, tcool = 3d21· 8h)

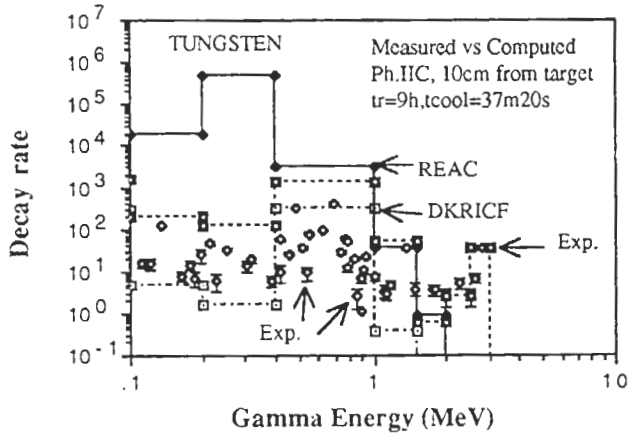

Figure 5f: Decay γ emission rate spectra per g from Tungsten Measurement vs. Computation

IV.I. Tungsten

^{187}W, ^{186}Ta and ^{183}Hf dominate short cooling time measurements. For larger cooling times, predominant contributor ^{187}W is backed up by ^{183}Ta and ^{182}Ta. One sample indicates the presence of Na/Al/Mg impurity. Tabulated γ-yield data[17] does not match with measured relative ratios for various γ peaks emitted by ^{186}Ta and ^{183}Hf. Further investigation is called for. DKRICF lacks decay data for ^{186}Ta, ^{187}W and ^{181}W. REAC analysis shows ^{179m}W ($t_{1/2}$=6.4m, 0.03% 289 KeV, 0.19% 282 KeV, 0.22% 239 KeV, 0.32% 120 KeV and 0.61% 102 KeV) as making dominant contributions for both short and long cooling times; γ-yield data is 2 to 3 orders higher in decay data library of REAC2. Also, ^{182m}Hf, ^{184}Ta, ^{183}Hf, ^{180m}Hf are strongly overestimated by REAC. γ-yields are found to be grossly overestimated for many products in THIDA.

IV.J. Tantalum

^{180m}Ta, ^{180m}Hf and ^{182}Ta dominate identifiable contributions to measured data. There are unidentified peaks at 110, 117, 148, 482, 500 and 1001 KeV. REAC strongly overestimates in 0.2-0.4 MeV (factor of 5) and 0.4-1.0 MeV (factor of 7) energy ranges.

IV.K. $YBa_2Cu_3O_7$

^{135m}Ba($t_{1/2}$=28.7h),^{139}Ba, $^{135m+g}$Xe and ^{90m}Y make largest identifiable contributions at short cooling times. There appears to be ^{87m}Sr peak at 388 KeV. Other contributors include ^{65}Ni, ^{62}Cu, ^{62m}Co, ^{64}Cu and ^{88}Y. At larger cooling times, ^{88}Y dominates the scene. REAC lacks decay data for ^{139}Ba, ^{133m}Ba, ^{135m}Ba and $^{135m+g}$Xe. DKRICF lacks decay data for Ba, Xe and Y. C/E ratios for ^{65}Ni, ^{62}Cu and ^{62m}Co deviate considerably from unity even though they are not crucial contributors to overall decay γ-emission rates.

V. CONCLUSIONS

Integrated and spectral decay γ-emission rates from fusion neutron induced radioactive materials have been measured and computed using four leading radioactivity codes. Large discrepancies have been revealed for many materials even for integrated rates. These materials include Ni, Mo, V, Ti, W, MnCu alloy, Cr, Si, In, Ta, Co, $YBa_2Cu_3O_7$ and Zr. Larger discrepancies are observed for spectral rates for practically all the materials. Inadequate experimental statistics is partly to blame in so far as contributions from weaker neutron-induced reactions are concerned. Largely, it is activation cross-sections and decay data that are inadequate and need large scale improvement. C/E results from THIDA are found to be most promising as a whole. RACC broadly follows DKRICF results though there are significant differences when it comes to the details of the spectral rates. Regarding both REAC and DKRICF, it is to be said that γ–yield data needs further improvement, though former scores over the latter in many respects. DKRICF lacks yield data for gamma peaks lying above 2.5 MeV except for some well-known exceptions. A thorough updating is required. Also, in general, the activation cross-sections for (n,γ) reactions need improvement as there is a systematic trend for larger C/E in softer spectra obtaining at '82cm' location.

DKRICF related observations meriting immediate attention follow: γ–yield data is missing for a large number of isotopes. For example, decay data is absent for Y, ^{186}Ta, ^{187}W, ^{181}W, Ba and Xe. For MnCu alloy, ^{62}Cu was overestimated by a factor of 3. For V, ^{48}V contribution is strongly overestimated. For Zr, ^{91m}Y contribution is severely underestimated.

REAC related observations can be summarized as follows: For V, ^{48}Sc and ^{49}Cr are strongly overestimated. For Ni, ^{57}Co, ^{58}Co, ^{59}Fe are too much overestimated. For Mo, ^{91}Mo is strongly overestimated and ^{101}Mo, ^{99}Mo, ^{98m}Nb, ^{97}Nb, ^{93m}Nb are underestimated. For MnCu alloy, ^{62}Cu is overestimated by as much as by a factor of 3. For Zr, ^{89m}Y decay/cross-section data needs early look. The discrepant data leads to large and unconvincing

overestimation. Also, ^{89}Zr and ^{91m}Y are strongly overestimated. For W, ^{179m}W yields abnormally large contribution for both short and long cooling times; major factor appears to be γ-yield data which is 2 to 3 orders higher. In addition, both decay and activation cross-section data for ^{182m}Hf, ^{184}Ta, ^{183}Hf and ^{180m}Hf need attention for doing away with strong overestimation.

Decay heat released in the form of γ's is directly calculable from the experimental data analyzed in this work. We have evaluated this quantity too. The broad C/E trends are similar to those for total decay γ-rates produced in Tables 3a to 3d, even though, the products with harder γ spectra gain upper hand. However, the analysis reported herein is more helpful in deciphering the problem radioactive products, and, of course, the decay/cross-section data of the radioactivity codes used for the analysis.

ACKNOWLEDGEMENTS

This effort is supported by the United States Department of Energy, Office of Fusion Energy under Grant No. DE-F603-86ER52124.

REFERENCES

1. D.L. HENDERSON and O. YASAR, "A Radioactivity and Dose Rate Calculation Code Package," Vol. 1 and 2, RSIC computer code collection, CCC-323 (April 1987).

2. J. JUNG, "Theory and Use of the Radioactivity Code RACC," ANL/FPP/ TM-122, Argonne National Laboratory (1979).

3. F. M. MANN, "REAC*2: Users Manual and Code Description, " WHC-EP-0282, Westinghouse Hanford Company (1989).

4. Y. SEKI et al., "THIDA-2: An Avanced Code System for Calculation of Transmutation, Activation, Decay Heat and Dose Rate," RSIC computer code collection, CCC-410 (April 1987).

5. K. TOMABECHI, "International Thermonuclear Experimental Reactor, ITER, " Fusion Engineering and Design , 8, 43 (1989)

6. J. DARVAS, "The European Fusion Nuclear Technology Effort," Fusion Engineering and Design, 8, 61 (1989).

7. S. TAMURA and FER design team," Design Study of Fusion Experimental Reactor at JAERI," Fusion Engineering and Design, 8, 29 (1989).

8. A. KUMAR et al., "Radioactivity and Nuclear Heating Measurements for Fusion Applications," paper presented at 16th symposium on fusion technology held 3-7 September, 1990, Abingdon, U.K.

9. Y. IKEDA et al., "Experiments on Induced Activities related to Decayheat in Simulated D-T Neutron Fields: JAERI/USDOE Collaborative Program on Fusion Neutronics Experiments," paper to be presented at this meeting.

10. Y. OYAMA et al., "Measured Characteristics of Be Multi-layered and Coolant Channel Blankets: Phase IIC Experiments of the JAERI/USDOE Collaborative Program on Fusion Neutronics," paper to be presented at this meeting.

11. M.Z. YOUSSEF et al., "Analysis for Heterogeneous Blankets and Comparison to Measurements: Phase IIC Experiments of the USDOE/JAERI Collaborative Program on Fusion Neutronics," paper to be presented at this meeting.

12. H. BABA, "Gamma-ray Spectrum Analysis Code for Ge(Li) Detectors," RSIC code package PSR-84 (1978); also, JAERI-M 7017, Japan Atomic Energy Research Institute (1977).

13. J.F . BRIESMEISTER, editor, "MCNP- A General Monte Carlo Code for Neutron and Photon Transport: Version 3A," report no. LA-7396-M, Rev. 2 (Sep. 1988), alongwith MCNP3B newsletter dated July 18, 1988, Los Alamos National Laboratory.

14. L.P. KU and J. KOLIBAL, "RUFF- A Ray Tracing Program to Generate Uncollided Flux and First Collision Moments for DOT 4, A User's Manual, EAD-R-16, Plasma Physics Laboratory, Princeton University (1980).

15. W.A. RHOADES and R. L. CHILDS, "DOT-IV Version 4.3: One and Two Dimensional Transport Code Collection, CCC-429 (May 1984).

16. Y. IKEDA et al., "Measurements of Induced Activity in Type 316 Stainless Steel by Irradiation in D-T Neutron Fields," Fusion Technology, 8, 1466 (1985).

17. C.M. LEDERER and V. SHIRLEY, editors, "Table of Isotopes," 7th edition, John Wiley & Sons, Inc., New York (1978).